JJEE

Volume 12 | Number 2 | June 2026 | Pages 399-415

Jordan Journal of Electrical Engineering

ISSN (print): 2409-9600, ISSN (online): 2409-9619

Homepage: jjee.ttu.edu.jo

Enhanced Direct Torque Control of DFIM Using an Intelligent Self-Adaptive Fuzzy Gain

Noreddine Choug[1*], Smail Dilmi[2]

[1] Electrical Engineering Laboratory (LGE), Electrical Engineering Department, Faculty of Technology. University of M'Sila, University Pole, Road Bordj Bou Arreridj M'sila 28000, Algeria
E-mail: choug.noreddine@univ-msila.dz

[2] LASS, Laboratory of Analysis of Signals and Systems, Electrical Engineering Department, Faculty of Technology.University of M'Sila, University Pole, Road Bordj Bou Arreridj M'sila 28000, Algeria

Received: Dec 22, 2025 *Revised: Jan 12, 2026* *Accepted: Mar 05, 2026* *Available online: Jun 15, 2026*

***Abstract*—** This article presents a cutting-edge advanced control strategy designed to optimize the performance of Doubly Fed Induction Motors (DFIM), prevalent in industrial applications demanding precise speed and torque regulation. Our approach combines Direct Torque Control (DTC) with an intelligent Fuzzy Logic Controller (FLC), incorporating a dynamic gain adaptation mechanism. DTC is chosen for its ability to deliver ultra-fast torque response and robust performance by directly controlling electromagnetic torque and stator flux. However, to overcome the limitations of conventional DTC, such as torque and flux ripples, an FLC is integrated at the heart of the control loop. The innovation of this work lies in the integration of an automatic gain adaptation system within the fuzzy controller. This mechanism, forming an Adaptive Gain Fuzzy Controller (AGFC), adjusts the system's responsiveness in real-time based on operating conditions (speed error and its derivative), providing superior robustness against load disturbances and motor parameter variations. This adaptive approach ensures optimal performance across a wide range of operating conditions, making it ideal for demanding industrial applications.

***Keywords*—** Doubly fed induction motor (DFIM); Direct torque control (DTC); Fuzzy logic controller (FLC); Adaptive gain fuzzy controller (AGFC).

1. INTRODUCTION

Electric motors play a crucial role in modern industry, converting a significant portion of electrical energy into mechanical energy. These motors vary widely in type and performance requirements, depending on the specific application. Effective response to changes in set points, such as speed, position, and torque, is essential for optimal operation. The Doubly Fed Induction Machine (DFIM) has emerged as a popular choice for variable-speed applications, particularly in wind power generation and electromechanical energy conversion, as evidenced by the growing body of research in recent years [1-5]. A key advantage of the DFIM lies in its use of a power converter with a fractional rating compared to the generator's nominal power, resulting in significant cost reductions compared to competing topologies. This work focuses on developing numerical tools for designing control laws that optimize DFIM performance across its operating range.

Traditional torque control systems are broadly categorized into scalar and vector control. Scalar control, based on steady-state relationships, regulates the magnitude and frequency of voltage, current, and flux vectors, but does not control their instantaneous position during transients. In contrast, vector control, also known as Field-Oriented Control (FOC), utilizes

* Corresponding author
DOI: https://doi.org/ 10.5455/jjee.204-1766431607

dynamic state relationships to control not only the magnitude and frequency but also the instantaneous position of these vectors, ensuring optimal orientation in both steady-state and transient conditions [6-8].

Direct Torque Control (DTC), introduced in the mid-1980s, presents a compelling alternative to FOC for AC machines. Based on the direct determination of inverter switching states, DTC offers a simpler control scheme with reduced sensitivity to machine parameters. However, the variable switching frequency inherent in conventional DTC leads to significant torque and flux ripples, resulting in acoustic noise and degraded performance. While classical DTC (DTC-C) has been extensively studied over the past few decades due to its advantages over FOC, the use of hysteresis controllers for flux and torque regulation introduces high ripples and variable switching frequency, posing challenges for low-speed control [9-10].

To address these limitations, researchers have explored numerous advanced control strategies. These include the use of space vector modulation (DTC-SVM), model predictive control (MPC-DTC), and various artificial intelligence (AI) techniques. AI-based approaches, such as those employing Neural Networks (NN-DTC) and Sliding Mode Control (SMC-DTC), have shown promise in reducing ripples and improving robustness [11-13]. However, these methods can introduce significant computational complexity or require intricate tuning.

This article proposes a novel advanced control strategy that seeks a balance between performance and implementation simplicity. We aim to optimize the performance of DFIMs in demanding industrial applications by combining DTC with an intelligent fuzzy logic-based regulator, which incorporates a dynamic gain adaptation mechanism. DTC is chosen for its fast torque response and robust performance, directly controlling electromagnetic torque and stator flux. The integration of a Fuzzy Logic Controller (FLC) mitigates the ripples inherent in conventional DTC. The key innovation of this work lies in the implementation of an automatic gain adaptation system within the fuzzy controller, creating an Adaptive Gain Fuzzy Controller (AGFC). This mechanism adjusts the system's responsiveness in real-time based on operating conditions (speed error and its derivative), providing enhanced robustness against load disturbances and parameter variations. This adaptive approach ensures optimal performance across a wide range of operating conditions, making it ideal for demanding industrial applications.

2. MATHEMATICAL MODELLING OF THE DOUBLY FED INDUCTION MOTOR

The dynamic behavior of the doubly fed induction motor (DFIM) is characterized using the space vector formalism within the (α, β) reference frame [3, 10,14].

$$\dot{X} = AX + BU \tag{1}$$

$$X = [I_{s\alpha} \quad I_{s\beta} \quad \varphi_{s\alpha} \quad \varphi_{s\beta}] \quad U = [V_{s\alpha} \quad V_{s\beta} \quad V_{r\alpha} \quad V_{r\beta}]$$

$$A = \begin{bmatrix} -\frac{1}{\sigma}\left(\frac{1}{T_s}+\frac{1}{T_r}\right) & -\omega & \frac{1}{L_s.\sigma.T_r} & \frac{\omega}{L_s.\sigma} \\ \omega & -\frac{1}{\sigma}\left(\frac{1}{T_s}+\frac{1}{T_r}\right) & -\frac{\omega}{L_s.\sigma}\omega & \frac{1}{L_s.\sigma.T_r} \\ -R_s & 0 & 0 & 0 \\ 0 & -R_s & 0 & 0 \end{bmatrix}$$

For the purpose of drive control synthesis, the state-space model is established by considering the stator current components and stator flux components as the fundamental state variables.

$$B = \begin{bmatrix} \frac{1}{\sigma . L_s} & 0 \\ 0 & \frac{1}{\sigma . L_s} \\ 1 & 0 \\ 0 & 1 \end{bmatrix}$$

with $\sigma = 1 - \frac{M^2}{L_s . L_r}$, $T_s = \frac{L_s}{R_s}$ and $T_r = \frac{L_r}{R_r}$

The mechanical and the electromagnetic torque equations are given by:

$$J\, d\Omega/dt + f.\Omega = T_{em} - T_r \quad (2)$$

$$T_{em} = p\left(\varphi_{s\alpha} I_{s\beta} - \varphi_{s\beta} I_{s\alpha}\right) \quad (3)$$

Detailed machine parameters are provided in Table 1.

Table 1. Machine parameters.

Parameters	Values
Nominal power P_n	1.5 kW
Voltage	220/380 V
Frequency	50 Hz
Pole pairs P	2
Stator Resistance R_s	1.75 Ω
Rotor Resistance R_r	1.68 Ω
Stator Inductance L_s	0.295 H
Rotor Inductance L_r	0.104 H
Mutual Inductance M	0.165 H
Inertia J	0.0426 Kgm²

3. PRINCIPLE OF DIRECT TORQUE CONTROL

Direct Torque Control (DTC) offers a compelling approach to motor control by directly regulating the motor's torque through the strategic application of voltage vectors from the inverter, see Fig. 1. This method focuses on precise control of the stator flux and electromagnetic torque, typically achieved using hysteresis controllers. These controllers maintain both instantaneous values within a defined band around the desired setpoint.

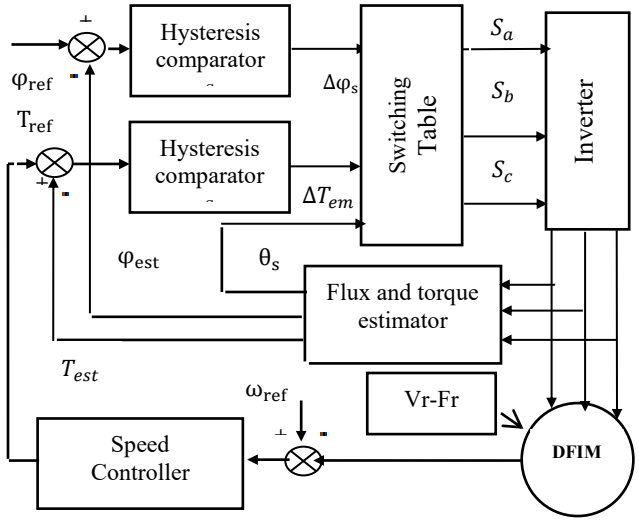

Fig. 1. Configuration of DTC in DFIM.

The output of these controllers then dictates the optimal inverter voltage vector to apply at each switching instant, resulting in highly responsive and dynamic motor performance. This approach distinguishes itself from traditional field-oriented control methods by directly controlling torque and flux, leading to potentially faster and more robust performance [15-18].

3.1. Stator Flux and Torque Estimation

The measurement of flux and torque is estimated based on the stator currents and voltages. Based on the dynamics of induction motor in stator fixed reference frame, the stator flux can be written as in equation below [19-20]:

$$\begin{cases} \varphi_\alpha = \int_0^t (V_{s\alpha} - R_s . I_{s\alpha}) dt \\ \varphi_\beta = \int_0^t (V_{s\beta} - R_s . I_{s\beta}) dt \end{cases} \quad (4)$$

The stator flux module can be calculated based on the flux components in the α-β coordinates, which can be mathematically defined as:

$$\varphi_s = \sqrt{\varphi_{s\alpha}^2 + \varphi_{s\beta}^2} \quad (5)$$

Then, the position of the stator flux is evaluated as:

$$\theta_s = atan\left[\frac{\varphi_{s\beta}}{\varphi_{s\alpha}}\right] \quad (6)$$

Meanwhile, the electromagnetic torque can be expressed as the difference of the product of the stator current and flux between different frames, as in the equation below:

$$\{T_{em} = p.(\varphi_{s\alpha} I_{s\beta} - \varphi_{s\beta} I_{s\alpha}) \quad (7)$$

3.2. Control of Stator Flux and Electromagnetic Torque

The magnitudes of the commanded stator flux φ_s and electromagnetic torque T_{em} are compared against their estimated counterparts. Resulting errors are then processed by independent two-level hysteresis comparators, one dedicated to flux and the other to torque. The digital outputs of the flux comparator follow the logic described below

$$\begin{cases} \Delta\varphi_s = 1 \ \ for \ |\varphi_s| \le \left|\varphi_{s-ref}\right| - |\Delta\varphi_s| \\ \Delta\varphi_s = 0 \ \ for \ |\varphi_s| \ge \left|\varphi_{s-ref}\right| + |\Delta\varphi_s| \end{cases} \quad (8)$$

The rotor reference speed is compared with the feedback speed and by suitable PI controller. This error is converted into reference torque. The digital outputs of the torque controller have following logic:

$$\begin{cases} \Delta T_{em} = 1 \ \ for \ |T_{em}| \le \left|T_{em.ref}\right| - |\Delta T_{em}| \\ \Delta T_{em} = -1 \ \ for \ |T_{em}| \ge \left|T_{em.ref}\right| + |\Delta T_{em}| \\ \Delta T_{em} = 0 \ \ for \\ \left|T_{em.ref}\right| - |\Delta T_{em}| \le |T_{em}| \le \left|T_{em.ref}\right| + |\Delta T_{em}| \end{cases} \quad (9)$$

3.3. Switching Table

The Selection of the voltage vector is dependent on the flux and torque errors as shown in Fig. 2 and Table 2.

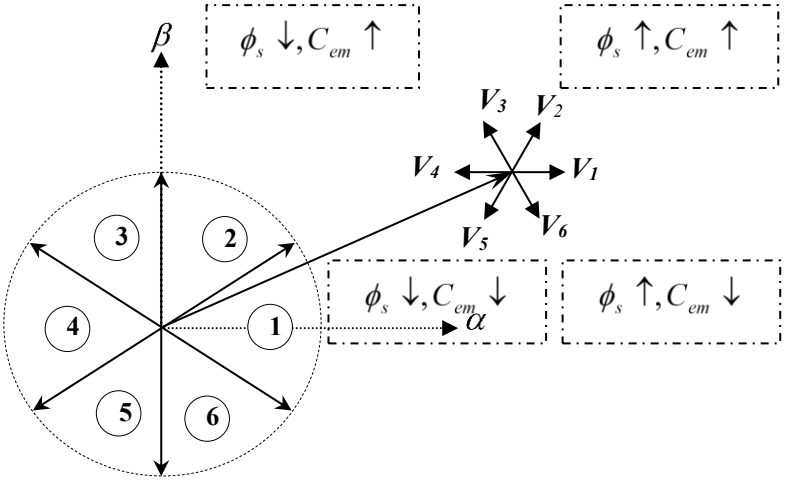

Fig. 2. Choosing the appropriate voltage vectors.

Table 2. Switching table.

$\Delta\varphi_s$	ΔT_{em}	S_1	S_2	S_3	S_4	S_5	S_6
0	1	011	011	001	101	100	110
	0	000	111	000	111	000	111
	-1	001	101	100	110	011	011
1	1	110	100	011	001	101	100
	0	111	000	111	000	111	000
	-1	101	100	110	011	011	001

4. CONTROLLERS SYNTHESIS

4.1. IP Speed Control of DFIM

The block diagram of the IP controller system is presented in Fig. 3.

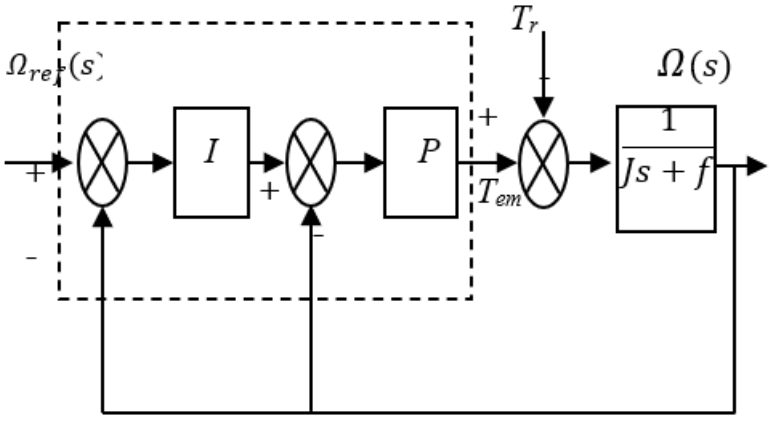

Fig. 3. IP Control speed of DFIM.

For mechanical quantity regulation, a Proportional-Integral (PI) type controller, modified into an Integral-Proportional (IP) controller, is employed. This modification offers the advantage of a zero-less closed-loop transfer function [21-22].

$$H(s) = \frac{1}{\frac{J}{K_p K_i}s^2 + \frac{K_p + f}{K_p K_i}s + 1} \quad (10)$$

To control the closed-loop system, appropriate selection of the coefficients K_P and K_i is crucial. Two methods can be used: pole compensation or pole placement, the latter of which will be employed in the following section.

The transfer function of a second-order closed-loop system is characterized by:

$$F(s) = \frac{1}{\frac{1}{{\omega_n}^2}s^2 + \frac{2\xi}{\omega_n}s + 1} \tag{11}$$

By comparing Eqs. (11) and (12), we find:

$$\begin{cases} \frac{J}{K_p K_i} = \frac{1}{{\omega_n}^2} \\ \frac{K_p + f}{K_p K_i} = \frac{2\xi}{\omega_n} \end{cases} \Rightarrow \begin{cases} K_p = 2J\xi\omega_n - f \\ K_i = \frac{J{\omega_n}^2}{K_p} \end{cases} \tag{12}$$

The controller gains are determined to achieve a minimal response time while ensuring no overshoot. This technique involves imposing values for ξ (damping ratio) and ω_n (natural frequency) to determine the coefficients K_p and K_i.

4.2. Fuzzy Speed Control of a DFIM

Fuzzy Logic Control (FLC), particularly well-suited for controlling complex systems with nonlinear or uncertain dynamics, offers a robust alternative to traditional control methods that require precise mathematical models. This characteristic makes FLC ideal for regulating the speed of a DFIM. The proposed control system utilizes an FLC to generate the necessary electromagnetic torque for precise speed control [23-26]. This control strategy is illustrated in Fig. 4.

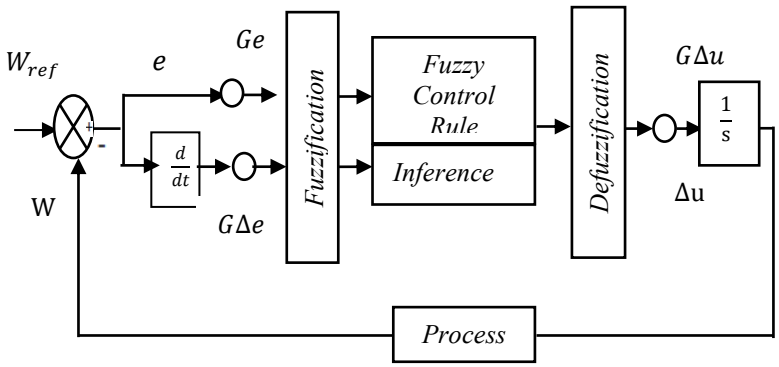

Fig. 4. Fuzzy logic control speed of DFIM.

In the above diagram, the inputs to the fuzzy controller are calculated at time step k as follows:

$$e(k) = \Omega_{ref}(k) - \Omega(\mathrm{k}) \tag{13}$$

Δe: The derivative of the error, approximated by:

$$\Delta e(k) = \frac{e(k) - e(k-1)}{T_e} \tag{14}$$

T_e: Is the sampling period

The output of the controller is given by:

$$T_{em}(k) = T_{em}(k-1) - \Delta u(k) \tag{15}$$

The gains $G_e, G_{\Delta e}, G_{ce}$are scaling factors that allow adjusting the sensitivity of the fuzzy controller without modifying the fuzzy structure. They serve to transform the physical values of the inputs into a normalized domain [-1, 1], referred to as the universe of discourse. Triangular and trapezoidal membership functions, as depicted in Fig. 5, are chosen for each

variable. The variables are normalized within a universe of discourse consisting of seven linguistic classes:

Z : Zero, NP : Negative Small, NG : Negative Large, PG : Positive Large, PP : Positive Small.

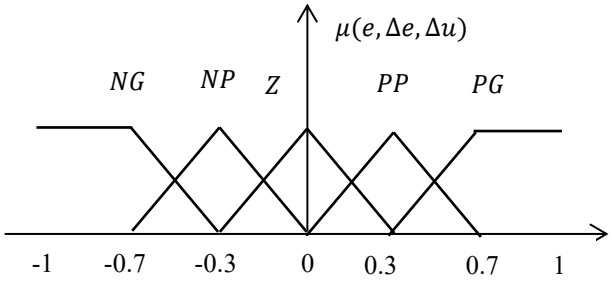

Fig. 5. Membership functions for input variables,e, Δe and output Δu.

To simplify the description of the inferences, we use an inference matrix, see Table 3.

Table 3. Basis for tuning the speed controllers.

$e, \Delta e$	NG	NP	Z	PP	PG
NG	PG	PG	PP	Z	NP
NP	PG	PP	PP	Z	NP
Z	PP	PP	Z	NP	NP
PP	PP	Z	NP	NP	NG
PG	Z	NP	NP	NG	NG

The inference method employed is the Max-Min method due to its ease of implementation. For defuzzification, the centroid (center of gravity) method is utilized, resulting in the following equation

$$dT_{em} = \frac{\sum_{i=1}^{n} \mu(dT_{em_i}) dte_i}{\sum_{i=1}^{n} \mu\,(dT_{em_i})} \tag{16}$$

n: the number of rules.

4.3. Fuzzy regulation with Self-Adaptive Gain

Problem Addressed

A fixed gain in the fuzzy controller can lead to poor performance, especially during transients (start-up, load changes, etc.). To improve stability and responsiveness, the control increment gain is itself made adaptive, using a secondary fuzzy logic controller, based on the system's instantaneous error and error variation [27]. The adaptive gain rule base presented in Table 4 and the membership functions shown in Fig. 6 were designed using a physically motivated heuristic approach. The design follows the basic control principle that large speed errors and rapidly changing errors require strong control action, whereas small errors near steady-state conditions require a reduced gain to avoid oscillations. The rule base was initially constructed using control-system insight and DFIM dynamics, and then refined through simulation-based tuning to minimize torque ripple and overshoot while ensuring fast transient response. Respond intelligently to varying conditions, optimizing performance and maintaining stability.

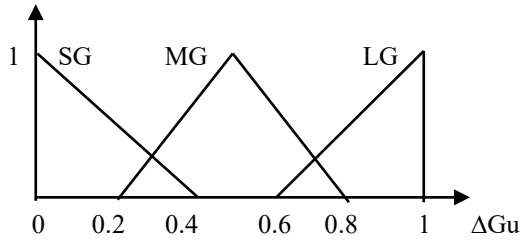

Fig. 6. Memberships function of control gain.

Table 4. Decision table for adaptive gain in fuzzy controller.

e / Δe	NG	NP	Z	PP	PG
NG	LG	LG	MG	SG	SG
NP	LG	MG	MG	SG	SG
Z	MG	MG	SG	MG	MG
PP	SG	SG	MG	MG	LG
PG	SG	SG	MG	LG	LG

Figure 7 depicts the fuzzy controller with the incorporated control gain adaptation. To enhance clarity and facilitate comprehension, a simplified representation of this controller is provided in Fig. 8.

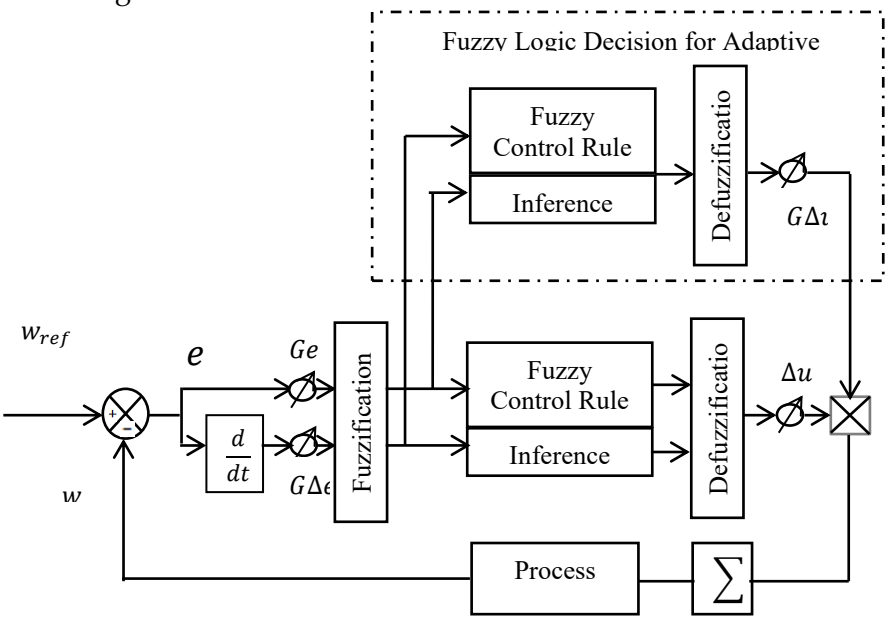

Fig. 7. Fuzzy controller with adaptive fuzzy gain.

Adaptive Gain Principle

- Adaptive gain GΔu.
- variable computed at each step by a secondary FLC.
- Inputs: Same as main FLC (e Δe).
- Output: Gain factor applied to the control increment Δu.
- Rule Base: Specific decision Table 4

New Control Law: $\boldsymbol{U_{k+1} = U_k + G_{\Delta U_{k+1}} * \Delta U_{k+1}}$

Inputs: Measured speed and reference are compared to compute the error and its variation.

Main FLC: Generates a control increment.

Secondary FLC: Computes an adaptive gain.

Multiplication: The adaptive gain modulates the control increment.

Integration/Update: Updates the command signal.

Actuator: Applies the computed command torque to the DFIM

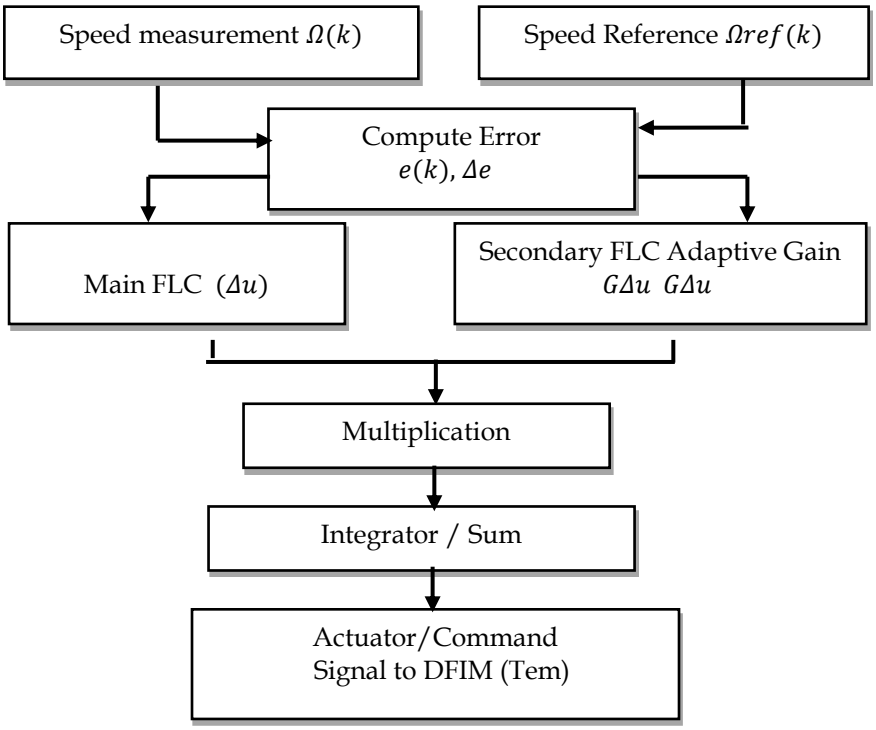

Fig. 8. Simplified representation of the fuzzy controller with adaptive gain.

The advantages of having a variable gain are :

- Improved stability during transients.
- Controller adaptation to different operating conditions.
- Robustness to parameter variations.

4.4. Implementation Challenges and Practical Considerations

In practical implementations of the proposed Adaptive Gain Fuzzy Controller (AGFC), several non-ideal effects must be considered, particularly measurement noise and inverter delays. The derivative of the speed error,

$$\Delta e(k) = \frac{e(k) - e(k-1)}{T}$$

Is highly sensitive to noise in the measured speed signal. In real drive systems, encoder quantization and electrical noise can introduce high-frequency fluctuations in Δe, which may cause undesired oscillations in the adaptive gain. To mitigate this effect, a low-pass filtered derivative is applied:

$\Delta ef(k) = \alpha \Delta ef(k-1) + (1-\alpha)\Delta e(k),\ where\ 0 < \alpha < 1.$

This filtering improves the robustness of the adaptive gain mechanism while preserving fast transient response. In addition, practical inverters introduce switching and computation delays, approximately equal to one sampling period plus PWM delay. These delays reduce the effective bandwidth of the torque control loop. However, in the proposed AGFC, an increase in tracking error automatically leads to a higher adaptive gain, which compensates for these delays and maintains fast dynamic response

5. COMPUTATIONAL COMPLEXITY AND REAL-TIME FEASIBILITY

The proposed AGFC introduces additional computational complexity compared to conventional DTC and single FLC schemes, since two fuzzy inference systems are executed at each sampling period. However, both fuzzy controllers use simple triangular membership functions and Max–Min inference with centroid defuzzification, resulting in linear computational complexity with respect to the number of rules. Modern DSP used in industrial motor drives are capable of executing several million floating-point operations per second. Therefore, the execution of two fuzzy controllers, together with flux and torque estimation, can be achieved within a typical DTC sampling period (50–100 μs), making the proposed control strategy suitable for real-time implementation.

6. SIMULATION RESULTS AND DISCUSSIONS

This section presents a thorough comparative analysis of three speed control strategies for the DTC-driven DFIM: IP control, standard FLC, and the proposed FLC with adaptive gain (AGFC). The study aims to identify the most effective strategy by evaluating the dynamic and static performance of each controller under various operating conditions. Detailed machine parameters are provided in Table 1. The following tests were performed:

- **Speed Reversal Test:** To evaluate transient performance and tracking capability.
- **Load Torque Variation Test:** To assess disturbance rejection capabilities.
- **Robustness Test:** To check performance under motor parameter variations.

6.1. Speed Reversal Test

This test evaluates the speed and smoothness of the motor's rotation reversal. The speed command is changed from 150 rad/s to -150 rad/s at t=1.5s. Figs. 9-13 illustrate the system's response. The AGFC is expected to provide the best performance, achieving a faster reversal with fewer oscillations and lower torque ripple.

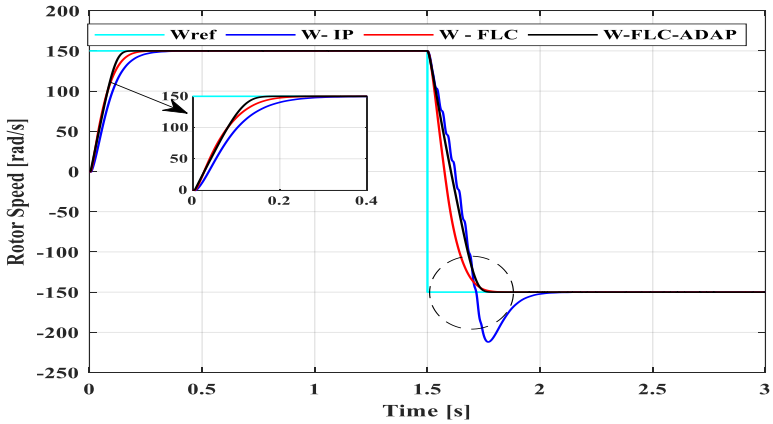

Fig. 9. Mechanical speed.

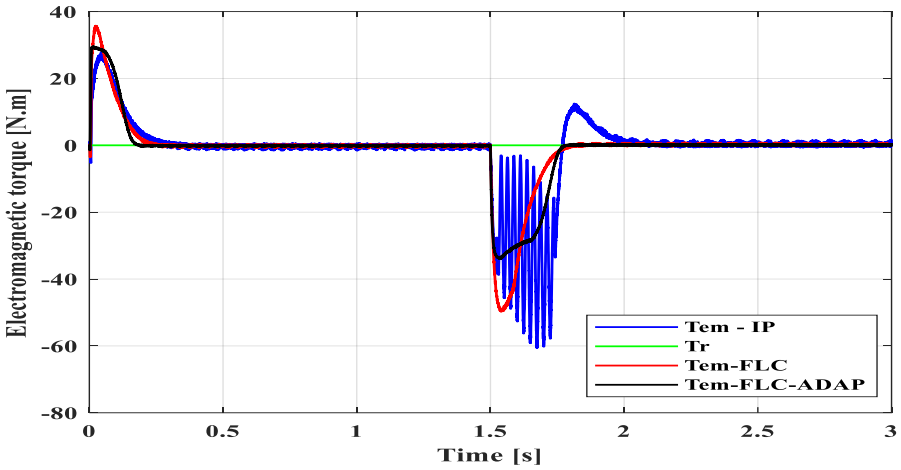

Fig. 10. Electromagnetic torque.

As seen in Fig. 9, the IP controller exhibits significant overshoots and a longer settling time. The FLC improves upon this, but the AGFC provides the fastest and smoothest response with no overshoot. Figure 10 shows the electromagnetic torque; the ripples are highest for the IP controller, reduced for the FLC, and minimized for the AGFC.

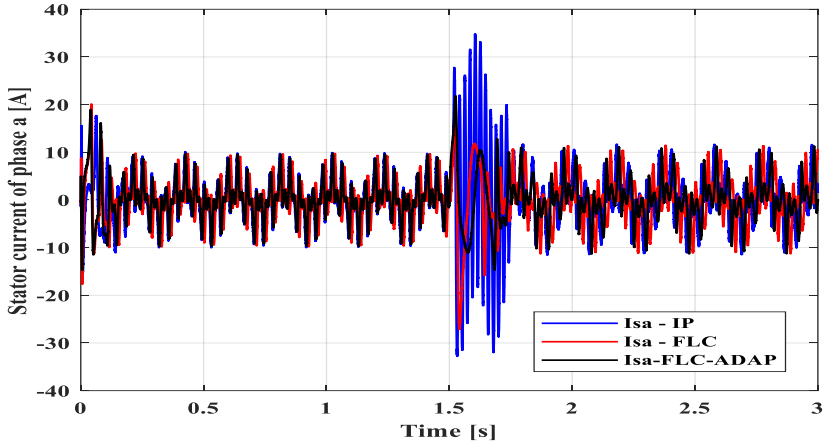

Fig. 11. Stator current of phase a.

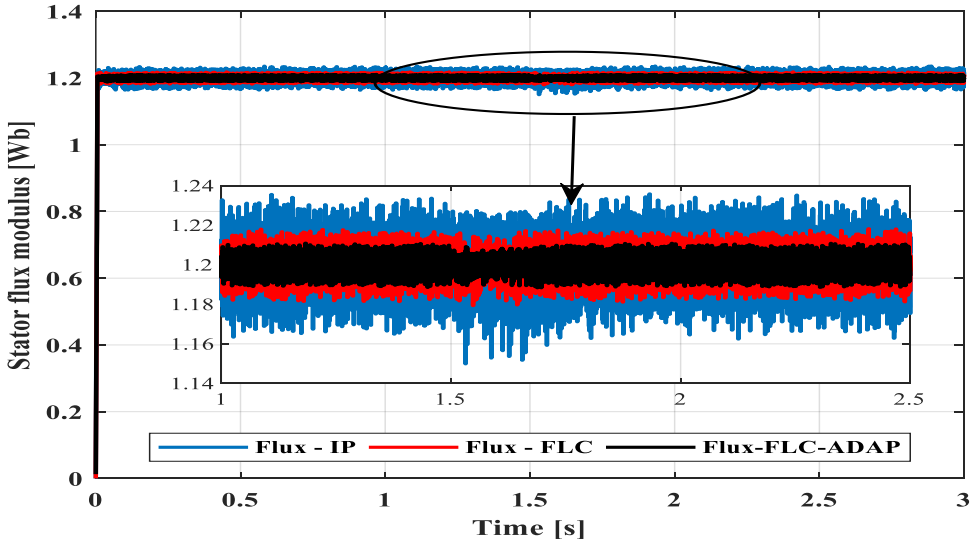

Fig. 12. Stator Flux Module.

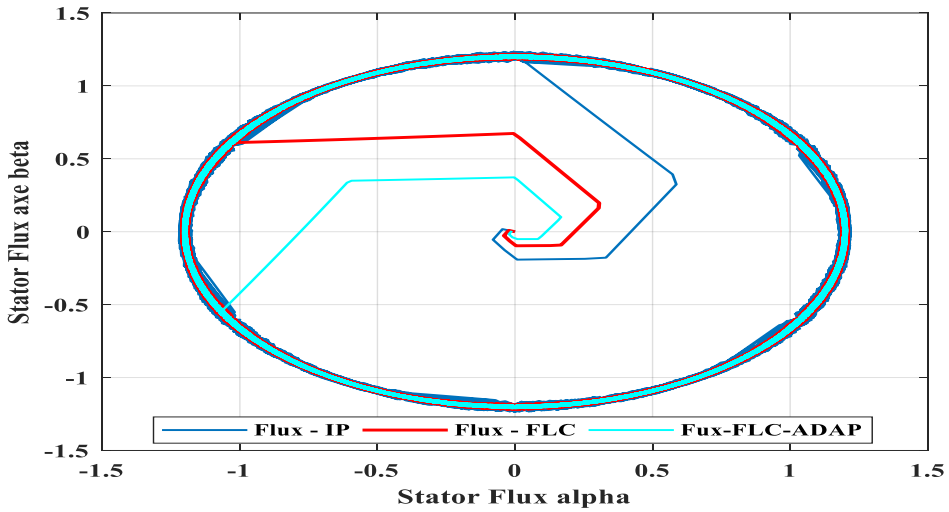

Fig. 13. Flux circular trajectory.

This demonstrates the AGFC's ability to provide strong torque for acceleration while maintaining smooth operation. The stator flux (Fig. 12) is kept within its hysteresis band for all controllers, but the AGFC shows the tightest regulation. Consequently, the stator flux trajectory (Fig. 13, shown for AGFC) is nearly perfectly circular, indicating excellent flux control

6.2. Load Torque Variation Test

This test assesses the system's robustness to external disturbances. At t=1s, a load torque of 5 Nm is applied, and at t=2s, it is increased to 10 Nm. Figures 14 and 15 show the system's response. The IP controller suffers a large speed drop and slow recovery.

The FLC performs better, but the AGFC demonstrates superior disturbance rejection, with a minimal speed drop and very fast recovery. This is because the adaptive gain increases to counteract the error caused by the load. The flux magnitude and trajectory (Figs. 16 and 17) remain stable, especially for the AGFC, proving its robustness.

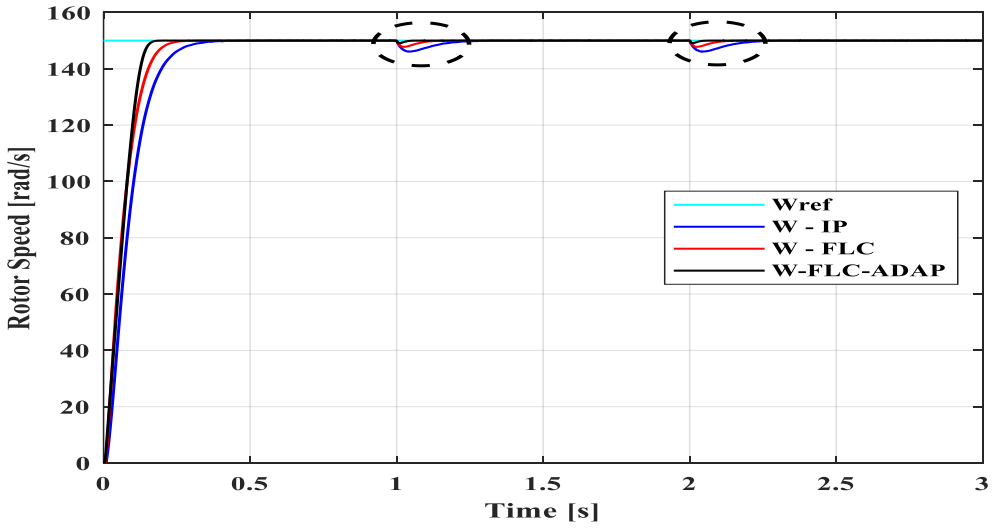

Fig. 14. Mechanical speed.

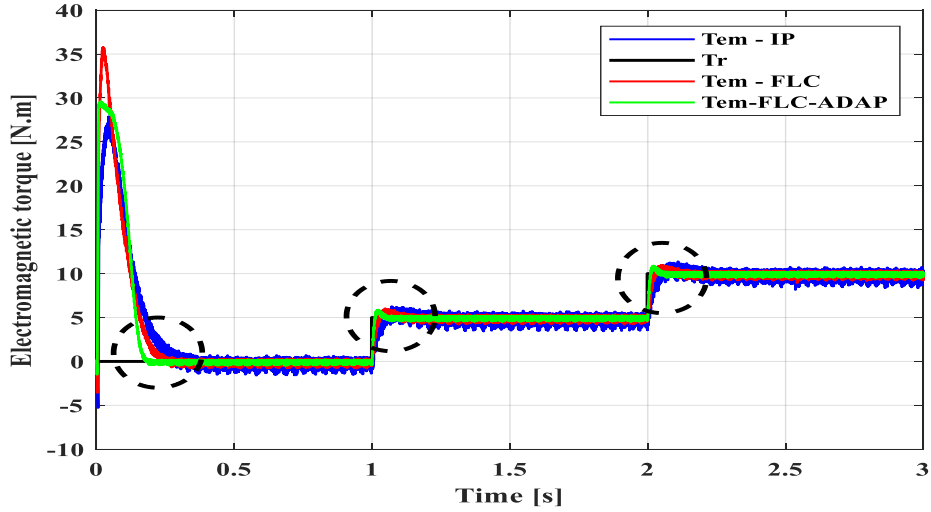

Fig. 15. Electromagnetic torque.

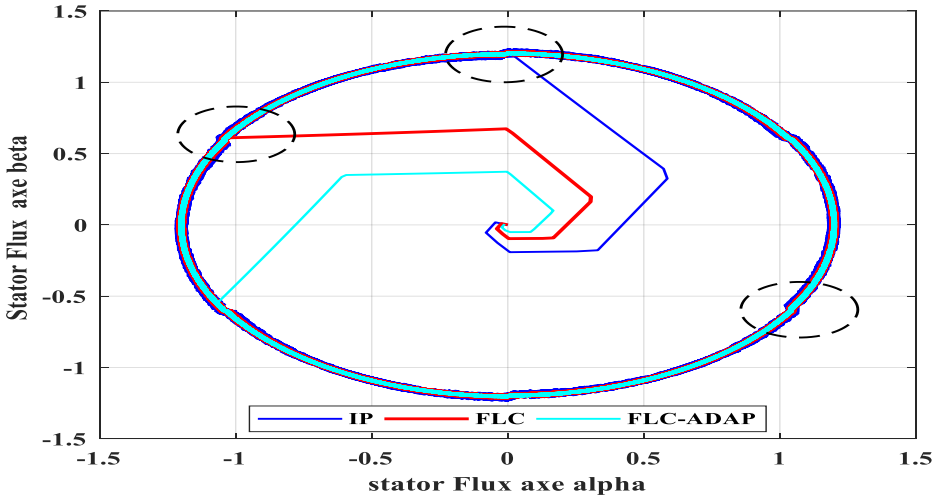

Fig. 16. Flux circular trajectory.

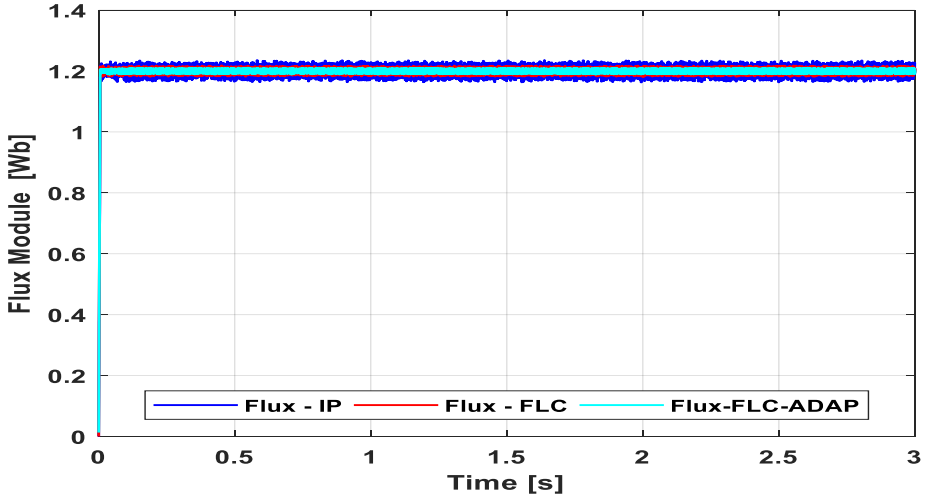

Fig. 17. Stator flux module.

6.3. Robustness Test Against Parameter Variation

A robustness test was performed at a reference speed of 40 rad/s under a 5 Nm load. At t = 2 s, the stator resistance Rs was increased by 50% to evaluate the controller's adaptability

to parameter variations. As shown in Fig. 18, the IP controller exhibits a significant steady-state speed error and slow recovery, indicating high sensitivity to resistance mismatch. The conventional FLC shows improved robustness but still suffers from noticeable speed oscillations. In contrast, the proposed AGFC maintains accurate speed tracking with minimal performance degradation.

The corresponding electromagnetic torque responses in Fig. 19 confirms these observations. The IP controller produces large torque ripple, while the FLC reduces oscillations but remains affected by the parameter change. The AGFC achieves smoother torque with reduced ripple, demonstrating superior robustness under stator resistance variation.

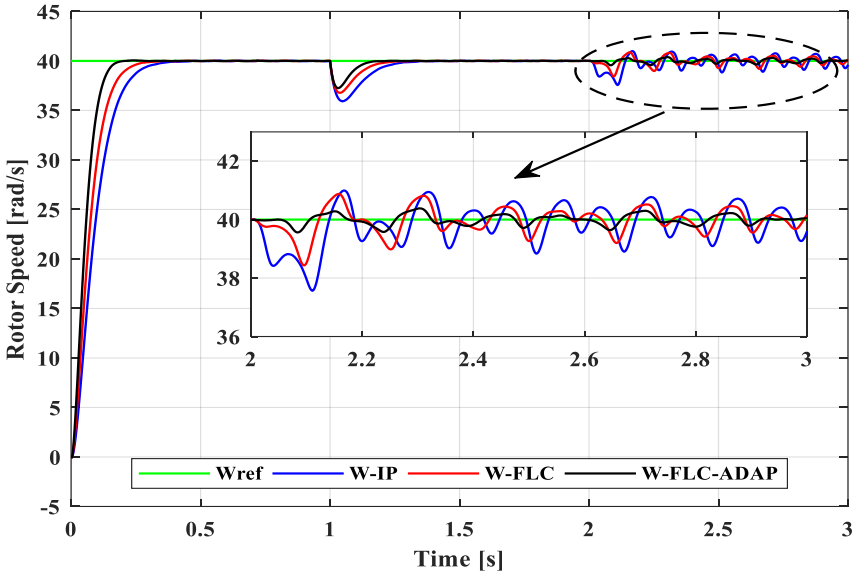

Fig. 18. Mechanical speed.

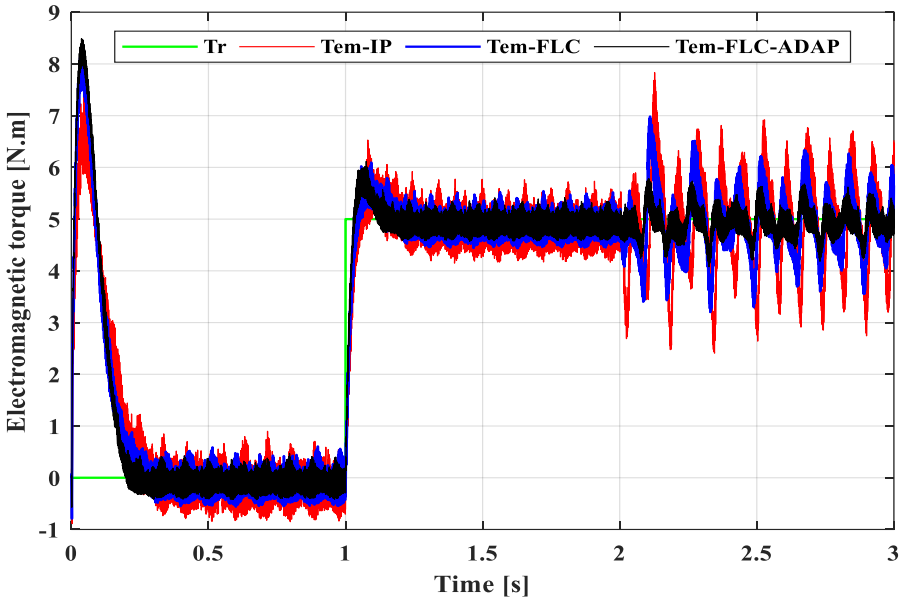

Fig. 19. Electromagnetic torque.

6.4. Quantitative Comparison

To better highlight the advantages of the proposed method, key performance indicators are extracted from the simulation results and summarized in Table 5. The results in Table 5

clearly quantify the superiority of the AGFC strategy. It achieves the fastest settling time with zero overshoot, exhibits the best load disturbance rejection (smallest speed drop and fastest recovery), significantly reduces torque ripple, and demonstrates the highest robustness against parameter variations.

Table 5. Controller quantitative performance comparison of controllers.

Performance metric	Test condition	IP	FLC	AGFC
Settling Time [s]	Speed Reversal	0.40	0.30	0.22
Speed Overshoot [%]	Speed Reversal	3.3%	1.3%	0%
Max Speed Drop [rad/s]	10 Nm Load	12.0	7.0	3.0
Recovery Time [s]	10 Nm Load	0.8	0.5	0.25
Torque Ripple [%]	Steady State	~20%	~12%	~6%
Speed Error [%]	Robustness Test	6.4%	3.8%	1.6%

7. CONCLUSIONS

This article introduced and validated a novel control strategy for Doubly Fed Induction Motors (DFIMs) by integrating Direct Torque Control (DTC) with an Adaptive Gain Fuzzy Controller (AGFC).

The AGFC delivers superior dynamic performance compared to conventional IP and standard FLCs, featuring faster settling times and reduced overshoot during speed reversals. It also exhibits remarkable robustness against sudden load disturbances and parameter variations, while ensuring smoother motor operation through a significant reduction in torque and flux ripples. Implementation of the proposed method presents several challenges. These notably include a high computational burden (due to the concurrent execution of two fuzzy controllers) and a strong reliance on expert knowledge for effectively defining the fuzzy rules and tuning the membership functions of the controller. Key areas for future research will focus on advancing this strategy. These include the application of this AGFC strategy to other types of AC machines and the automation of fuzzy controller tuning using robust optimization algorithms (e.g., Genetic Algorithms (GA), Particle Swarm Optimization (PSO)). Most critically, experimental validation on a dedicated laboratory test bench is essential to confirm the simulated results and assess the real-world efficacy of the AGFC.

Finally, developing more sophisticated adaptation mechanisms, potentially incorporating machine learning algorithms for online learning, will be explored to further enhance the controller's intelligence and performance.

REFERENCES

[1] K. Zergaw, M. Tuka, "Analysis of Voltage dip impact on doubly fed induction generator under dynamic conditions," *Jordan Journal of Electrical Engineering*, vol. 9, no. 3, pp. 338–356, 2023, doi: 10.5455/jjee.204-1669034454.

[2] M. El Mahfoud, B. Bossoufi, N. El Ouanjli, S. Mahfoud, M. Taoussi, "three speed controllers of direct torque control for a doubly fed induction motor drive–a comparison," *Electrica*, vol. 21, no. 1, pp. 129–141, 2021, doi: 10.5152/electrica.2021.20060.

[3] M. Tuka, "Investigation of voltage dip problems during faults on a grid-tied doubly fed induction generator in a wind energy system," *Jordan Journal of Electrical Engineering*, vol. 9, no. 2, pp. 209–227, 2023, doi: 10.5455/jjee.204-1669028936.

[4] N. El Ouanjli, S. Motahhir, A. Derouich, A. El Ghzizal, A. Chebabhi, M. Taoussi, "Improved DTC strategy of doubly fed induction motor using fuzzy logic controller," *Energy Reports*, vol. 5, pp. 271–279, 2019, doi: 10.1016/j.egyr.2019.02.001.

[5] R. Pandya, H. Jaydeep, G. Rajan, N. Hiral, "Doubly fed induction motor for speed control of motor," *Journal of Emerging Technologies and Innovative Research*, vol. 5, no. 4, pp. 322–325, 2018.

[6] O. Otkun, "Scalar speed control of induction motors with difference frequency," *Journal of Polytechnic*, vol. 23, no. 2, pp. 267–276, 2020, doi: 10.2339/politeknik.474043.

[7] K. Annuar, M. Sapiee, R. Nor, M. Azali, M. Shah, S. Rozali, "Squirrel cage induction motor scalar control constant V/F analysis," vol. 17, no. 1, pp. 417–424, 2019, doi: 10.12928/TELKOMNIKA.v17i1.8818.

[8] A. Agrawal, R. Lodhi, P. Nema, "Comparison between scalar and vector control technique for induction motor drive," *International Research Journal of Engineering and Technology*, vol. 5, no. 6, pp. 2504–2509, 2018.

[9] Y. Zahraoui, M. Akherraz, C. Fahassa, S. Elbadaoui, "Induction motor DTC performance improvement by reducing flux and torque ripples in low speed," *Journal of Robotics and Control,* vol. 3, no. 1, pp. 93–100, 2022, doi: 10.18196/jrc.v3i1.12550.

[10] N. Choug, S. Belkacem, S. Benaggoune, "Advanced direct torque control: employing fuzzy logic for dynamic and adaptive regulation," *Journal of Electrical Systems*, vol. 20, no. 3, pp. 9289–9300, 2024, doi: 10.52783/jes.8394.

[11] S. Gdaim, A. Mtibaa, M. Mimouni, "Artificial neural network-based DTC of an induction machine with experimental implementation on FPGA," *Engineering Applications of Artificial Intelligence*, vol. 121, p. 105972, 2023, doi: 10.1016/j.engappai.2023.105972.

[12] S. Mahfoud, A. Derouich, N. El Ouanjli, M. El Mahfoud, "Enhancement of the direct torque control by using artificial neuron network for a doubly fed induction motor," *Intelligent Systems with Applications*, vol. 13, p. 200060, 2022, doi: 10.1016/j.iswa.2022.200060.

[13] T. Belbekri, B. Bouchiba, I. Bousserhane, H. Becheri, "A study of sensorless vector control of IM using neural network luenberger observer," *International Journal of Power Electronics and Drive Systems*, vol. 11, no. 3, pp. 1259–1267, 2020, doi: 10.11591/ijpeds.v11.i3.pp1259-1267.

[14] B. Farid, B. Tarek, B. Sebti, "Fuzzy super twisting algorithm dual direct torque control of doubly fed induction machine," *International Journal of Electrical and Computer Engineering*, vol. 11, no. 5, pp. 3782–3790, 2021, doi: 10.11591/ijece.v11i5.pp3782-3790.

[15] H. Vo, D. Nguyen, Q. Nguyen, C. Dong, T. Tran, P. Brandstetter, "Pulse-width modulation direct torque control induction motor drive with kalman filter," *Telkomnik*, vol. 19, no. 1, pp. 277–284, 2021, doi: 10.12928/TELKOMNIKA.v19i1.16247.

[16] N. El Ouanjli, A. Derouich, A. El Ghzizal, S. Motahhir, A. Chebabhi, Y. El Mourabit, M. Taoussi, "Modern Improvement techniques of direct torque control for induction motor drives – a review," *Protection and Control of Modern Power Systems*, vol. 4, p. 11, 2019, doi: 10.1186/s41601-019-0125-5.

[17] Y. Wiam, H. Ali, "Direct torque control-based power factor control of a DFIG," *Energy Procedia*, vol. 162, pp. 296–305, 2019, doi: 10.1016/j.egypro.2019.04.031.

[18] F. Wang, J. Wang, L. Yu, "Robust time delay compensation for DTC-based induction machine systems via extended state observers," *Journal of Power Electronics*, vol. 18, no. 3, pp. 736–745, 2018, doi: 10.6113/JPE.2018.18.3.736.

[19] B. Aykut, A. Gelen, "Sensorless Direct torque control based on seven-level torque hysteresis controller for five-phase IPMSM using a sliding-mode observer," *Engineering Science and Technology, an International Journal*, vol. 24, no. 5, pp. 1134–1143, 2021, doi: 10.1016/j.jestch.2021.02.004.

[20] N. Aisyah, M. Azri, A. Jidin, M. Aihsan, "A new optimal DTC switching strategy for open-end windings induction machine using a dual-inverter," *International Journal of Power Electronics and Drive Systems*, vol. 12, no. 3, pp. 1405–1412, 2021, doi: 10.11591/ijpeds.v12.i3.pp1405-1412.

[21] O. Abdalla, M. El Korfolly, S. Elmasry, I. Htita, "Harmonics mitigation and reactive power compensation of variable speed drive using a multi-function converter system with pi controller tuned by horse herd optimization technique," *Jordan Journal of Electrical Engineering*, vol. 11, no. 3, pp. 565–586, 2025, doi: 10.5455/jjee.204-1745508806.

[22] H. Maghfiroh, M. Ahmad, A. Ramelan, F. Adriyanto, "Fuzzy-PID in BLDC Motor speed control using MATLAB/Simulink," *Journal of Robotics and Control*, vol. 3, no. 1, pp. 8–13, 2022, doi: 10.18196/jrc.v3i1.10964.

[23] N. Choug, S. Benaggoune, S. Belkacem, "Hybrid fuzzy reference signal tracking control of a doubly fed induction generator," *International Journal of Engineering Transactions A: Basics*, vol. 33, no. 4, pp. 567–574, 2020, doi: 10.5829/ije.2020.33.04a.08.

[24] A. Shaout, S. Ahmad, D. Osborn, "Comparison of fuzzy logic control and model predictive control for a smart adaptive cruise control vehicle system," *Jordan Journal of Electrical Engineering*, vol. 10, no. 1, pp. 27–47, 2024, doi: 10.5455/jjee.204-1687812578.

[25] S. Abdulla, "Comparative assessment of PID, fuzzy logic and ANFIS controllers in an automatic voltage regulator of a power system," *Jordan Journal of Electrical Engineering*, vol. 8, no. 4, pp. 379–394, 2022, doi: 10.5455/jjee.204-1664025424.

[26] A. Abu-Ghazal, Q. Jaber, "Comparative Analysis of Induction Motor and Interior Permanent Magnet Synchronous Motor in Electric Vehicles with Fuzzy Logic Speed Control," *Jordan Journal of Electrical Engineering*, vol. 5, no. 4, pp. 202–221, 2019.

[27] N. Choug, S. Benaggoune, S. Belkacem, "Fuzzy control with adaptive gain of DFIG based WECS," 4th International Conference on Artificial Intelligence in Renewable Energetic, 2020.